Low-density repulsive Fermi gas in two dimensions: Bound-pair excitations and Fermi-liquid behavior

Jan R. Engelbrecht
Department of Physics, University of Illinois at Urbana-Champaign, 1110 West Green Street, Urbana, Illinois 61801

Mohit Randeria
Materials Science Division, Argonne National Laboratory, 9700 South Cass Avenue, Argonne, Illinois 60439
(Received 29 July 1991)

We study the dilute-gas expansion for a two-dimensional Fermi system with arbitrary short-range repulsive interactions. In contrast with the three-dimensional case, we find an unusual pole in the vertex part in the particle-particle channel, for all center-of-mass momenta $q<2k_F$. We show that this represents an excitation consisting of bound hole pairs, which disperses down to zero energy at $q=2k_F$. We study the effect of these bound states on the single-particle self-energy and find that the quasiparticles are well defined. Thus in the low-density regime, there is no breakdown of Fermi-liquid theory. In the Appendix we discuss the two-particle phase shift in the dilute Fermi gas, its connection with bound states, and the analogy with the potential scattering phase shift.

I. INTRODUCTION

With the discovery of high-temperature superconductivity[1] in the layered copper-oxide materials, there is great interest in understanding strongly correlated fermion systems. The unusual properties of these materials above T_c have led to suggestions[2,3] that the normal state is not an ordinary Landau Fermi liquid. The extent to which the experiments force us to modify the traditional Fermi-liquid idea is a matter of some debate at the present time.[4] On the theoretical side, it would be nice to have examples of models in two or more dimensions which do not have a broken symmetry and yet show non-Fermi-liquid behavior. It is, of course, well known that one-dimensional (1D) interacting Fermi systems[5] are not ordinary Fermi liquids[6]—they show power-law singularities, instead of a discontinuity, at their Fermi surface, and there is a separation of the charge and spin degrees of freedom.

Anderson has recently suggested that the ground state of the 2D Hubbard model differs from a Landau Fermi liquid due to the existence of antibound states[7] which lead to a nonvanishing Fermi-surface phase shift[8] even in the low-density limit. If Fermi-liquid theory indeed breaks down in this limit, i.e., very far from half filling, then it should be possible to establish this fact unambiguously. First, unlike near half-filling, there are no other instabilities—antiferromagnetism, metal-insulator transition, Nagaoka ferromagnetism, etc.—to contend with. Second, in this regime one can make a continuum approximation for which there is a small parameter in which to make a systematic expansion. (Note that a low-density expansion is possible only for a Fermi system with short-range interactions. It is, of course, well known that the Coulomb system at low densities is a Wigner crystal.)

In this paper we study the following question: Is the low-density Fermi gas in 2D a Fermi liquid or does the two-dimensionality lead to nontrivial behavior? We find that, in spite of the occurrence of unexpected nonperturbative effects in 2D, the system has well-defined fermionic quasiparticle excitations. Thus, two-dimensionality alone is not sufficient to lead to a breakdown of Fermi-liquid behavior. Some of the results of this paper have been previously presented in Refs. 9 and 10.

In the remainder of this section we summarize our results and end with an outline of the paper. The model we study is a 2D Fermi gas with arbitrary short-range repulsive interactions where the interparticle spacing is very much larger than the range of the two-body interactions. The three-dimensional case—dilute gas of hard-sphere fermions—was studied in great detail many years ago[11–13] and provided an early example of a Landau Fermi liquid in which all the quantities of interest could be calculated systematically in an expansion in k_Fa, where a is the s-wave scattering length. Using a T-matrix analysis, we find the expansion parameter appropriate to 2D. For weak repulsion, the domain of validity of the low-density expansion is $k_FR \ll 1$, where R is the range of the potential; while for the case of a hard-disk potential of radius R, one is limited to $1/\log(1/k_FR) \ll 1$.

We study the vertex part in the particle-particle channel and find an unusual pole for all center-of-mass momenta $q<2k_F$ which do not exist in higher dimensions. At first sight, this pole, which is below the bottom of the two-particle band, might appear to indicate a breakdown of Fermi-liquid theory. However, we argue below that it is, in fact, a collective excitation of the system consisting of a bound pair of holes, which does not lead to either an instability (phase transition) or to a more subtle breakdown of Fermi-liquid theory, at least within the low-density regime. We show that these bound states lead to a $|\omega|^{5/2}$ correction to the standard 2D result[14] for the imaginary part of the single-particle self-energy $\Sigma''(k_F,\omega)\sim\omega^2\ln|\omega|$. Using analyticity, we argue that the

quasiparticle residue Z is nonzero. The effect of the bound states on the quasiparticles is weak due to the limited phase space available for scattering into these states and to the small spectral weight in the bound pole at low energies.

Working directly with the Hubbard model, Fukuyama, Narikiyo, and Hasegawa[15] have subsequently obtained results identical to ours for the self-energy within a T-matrix approximation. Using a completely different formalism, Mattis and Chen[16] have shown that the quasiparticle renormalization Z for the low-density Hubbard model is nonzero.

In a companion paper,[17] written in collaboration with Zhang, we address the issue of the Fermi-liquid parameters of the 2D Fermi gas. The occurrence of a pole in the vertex part means that certain vertices which are usually assumed to be regular in Landau Fermi-liquid theory are, in fact, singular in 2D. Nonetheless, we find[17] that the singularities are sufficiently weak that the f function describing the residual interaction between the quasiparticles is well behaved.

The rest of the paper is organized as follows. In Sec. II, we show how the vertex part of interest may be expressed in terms of the two-body scattering T matrix. We also discuss the region of validity of the low-density expansion in 2D. In Sec. III, we study the singularities of the vertex part in the particle-particle channel, and show the existence of the bound states in addition to the usual continuum of excitations. We then turn to the effect of the bound states on various quantities of interest. In Sec. IV, we study the phase shift characterizing two-body scattering in the system. In Sec. V, we use the phase shift to calculate thermodynamic functions like the ground-state energy and the chemical potential. In Sec. VI, we look at quasiparticle lifetimes and residues to check the validity of Fermi-liquid theory.

We discuss the physical significance of our results in Sec. VII, and comment on their relevance to some of the proposals for the breakdown of Fermi-liquid theory made in the recent literature. We contrast the 2D calculation with the one-dimensional case, and comment on the connection of our results with the rather different case[18–20] of attractive Fermi systems in 2D. Finally, in Sec. VIII, we summarize our conclusions.

In the Appendix, we discuss the analogies between the formalism used for the dilute Fermi gas and that for the problem of noninteracting fermions in the presence of an impurity potential. Since the only important interaction processes in the dilute Fermi system are two-particle collisions, in the presence of the medium, these are conveniently described by a two-body phase shift. The intuitive content of this phase shift is brought out by studying the analogies and differences between this phase shift and that of ordinary potential scattering theory.

II. MANY-BODY FORMALISM

We study a gas of fermions of 2D with a spin-independent repulsive two-body interaction whose range R is much less than the average interparticle distance k_F^{-1}. As discussed below, the shape of the potential can be completely arbitrary; we can even tolerate some attraction so long as it is weak enough not to lead to the formation of a bound state in vacuum. For simplicity we only consider potentials for which the low-energy T-matrix elements are dominated by the s-wave channel in the partial-wave expansion.

In this section we first review the T-matrix formalism for the two-body problem in 2D. We then obtain a formal expression for the vertex part in the particle-particle channel for the many-body system. Finally, we comment on the expansion parameter and region of applicability of the low-density expansion in 2D.

A. Two-particle scattering in vacuum

We begin by calculating the T matrix which describes the scattering of two fermions in a relative s-wave, spin-singlet state in the particle vacuum, i.e., the two-body problem. The diluteness condition $k_F R \ll 1$ in the many-body problem allows us to focus only on matrix elements of the low-energy T matrix between states with small wave numbers. In the many-body description it will be convenient to represent the particle interactions by this T matrix instead of the interaction potential, V. This not only allows us to deal with arbitrarily strong repulsion, e.g., hard cores, but also allows us to characterize the low-energy, long-wavelength, two-body interaction in terms of a simple, separable kernel.

The two-body problem has dynamics only in the relative coordinates and the T matrix is given by the Born series

$$T_{\mathbf{k},\mathbf{k}'}(\omega)=V_{\mathbf{k},\mathbf{k}'}+\sum_{\mathbf{p}} V_{\mathbf{k},\mathbf{p}}G_{\rm rel}(\mathbf{p},\omega)T_{\mathbf{p}',\mathbf{k}'}(\omega)\ , \qquad (1)$$

where $G_{\rm rel}(\mathbf{p},\omega)=(\omega-\hbar^2p^2/2m_0+i\eta)^{-1}$ is the relative coordinate propagator in vacuum with $m_0=m/2$ the reduced mass. Anticipating the many-body description, it is instructive to account for the center-of-mass variables explicitly and generalize the two-body T matrix of (1) to

$$T_{\mathbf{k},\mathbf{k}'}(\mathbf{q},\omega)=V_{\mathbf{k},\mathbf{k}'}+\sum_{\mathbf{p},\mathbf{p}'} V_{\mathbf{k},\mathbf{p}}\mathcal{K}^0_{\mathbf{p},\mathbf{p}'}(\mathbf{q},\omega)T_{\mathbf{p}',\mathbf{k}'}(\mathbf{q},\omega)\ . \qquad (2)$$

Here the kernel in the two-body problem represents the propagation of a pair of particles in vacuum with momenta $\pm\mathbf{p}+\mathbf{q}/2$; therefore,

$$\begin{aligned}\mathcal{K}^0_{\mathbf{p},\mathbf{p}'}(\mathbf{q},\omega)&=-i\int\frac{d\omega'}{2\pi}\frac{1}{\omega'-\varepsilon_{\mathbf{p}+\mathbf{q}/2}+i\eta}\\&\quad\times\frac{1}{\omega-\omega'-\varepsilon_{-\mathbf{p}+\mathbf{q}/2}+i\eta}\delta_{\mathbf{p},\mathbf{p}'}\\&=\frac{1}{\omega-\hbar^2p^2/2m_0-\hbar^2q^2/2M+i\eta}\delta_{\mathbf{p},\mathbf{p}'}\end{aligned} \qquad (3)$$

with the single-particle energy $\varepsilon_{\mathbf{k}}=\hbar^2k^2/2m$ and $M=2m$. This generalized T matrix of Eq. (2) clearly reduces to (1) in the limit $\mathbf{q}\to\mathbf{0}$. Diagrammatically, Eq. (2) may be represented by ladder diagrams with repeated two-particle scattering. Note that, since there are no particle-hole excitations in the particle vacuum, these diagrams exhaust all scattering possibilities in the two-body problem.

It will be seen that one can set $\mathbf{q}=0$ in (2) without loss of generality for our calculation, and thus we will solve the two-body problem in a frame where the center of mass is at rest. The on-shell T matrix for the two-body problem is given by

$$\tau_0(\omega)\equiv\frac{4\hbar^2}{mL^2}\frac{1}{-\cot\delta_0(\omega)+i}\ , \tag{4}$$

where L^2 is the size of the system. (See Ref. 19 for more details on 2D scattering theory.) Using the usual technique of matching wave functions at the interaction range R, it can be shown that the low-energy s-wave phase shift $\delta_0(\omega)$ in 2D is given by

$$\cot\delta_0(\omega)=(1/\pi)\ln(\omega/E_a)+O(\omega/\varepsilon_R)\ , \tag{5}$$

where $\varepsilon_R=\hbar^2/2mR^2$. Just as the 3D phase shift is described by the scattering length, in 2D it is characterized by a single parameter E_a with dimensions of energy. A general expression for E_a is given by $E_a=4\varepsilon_R\exp(-2\gamma+2/\beta_0)$, where γ is Euler's constant and β_0 is the logarithmic derivative of the $l=0$ wave function evaluated just inside in the range of the potential, and at zero energy.

Consider, for example, the potential $V(r)=V_0\Theta(R-r)$. It is easy to show that

$$E_a=a\varepsilon_R\exp[bxI_1(x)/I_0(x)],\quad x\equiv\sqrt{V_0/\varepsilon_R}\ , \tag{6}$$

where the $I_n(x)$ are modified Bessel functions, and a and b are constants of order unity. In the weak repulsion limit, $V_0\to 0$, the parameter E_a diverges exponentially, while for the opposite hard-core limit, $V_0\to\infty$, one finds $E_a\sim O(\varepsilon_R)$. Further, as shown in Ref. 19, the parameter E_a is greater than or of order the energy scale ε_R even if the potential has some attractive part—say, for instance, a "hard-core plus square-well" potential—provided the attraction is not strong enough to give rise to a two-body bound state in vacuum.

We shall thus consider effectively repulsive short-range potentials for which the parameter E_a characterizing the low-energy phase shift is greater than or of the order of the already large energy scale $\varepsilon_R=\hbar^2/2mR^2$. Thus, we have

$$E_a\gtrsim\varepsilon_R\gg\varepsilon_F\ . \tag{7}$$

We shall see below that, in fact, one needs a rather more stringent inequality $g\equiv 1/\ln(E_a/2\varepsilon_F)\ll 1$ for the validity of the low-density expansion.

The low-energy s-wave T matrix can be shown[19] to be independent of the momenta $\mathbf{k}$ and $\mathbf{k}'$ for $kR\ll 1$ and $k'R\ll 1$. Using the above results, we then obtain the T matrix in manifestly separable form

$$T_{\mathbf{k},\mathbf{k}'}(\omega)\approx\tau_0(\omega)\approx\frac{4\pi\hbar^2}{mL^2}\frac{1}{\ln|E_a/\omega|+i\pi\Theta(\omega)}\ . \tag{8}$$

The first approximation is valid in the small k and k' regime, and the second ignores terms of order (ω/ε_R). We see that, at low energies, the T matrix has a logarithmic singularity—the scattering amplitude vanishes logarithmically—which is characteristic of two dimensions. We will show below that, in the many-body problem, this logarithm is cutoff on the scale of the Fermi energy.

B. Two-body scattering in a medium

Now we turn to the many-body system: a degenerate Fermi gas with two-body interactions described by the T matrix of Eq. (8) at temperatures $kT\equiv 1/\beta\ll\mu$, where μ is the chemical potential. Unlike the two-body problem, the inclusion of all contributions to the perturbative expansion is an unattainable task. Progress can only be made by restricting the analysis to some class of diagrams which, hopefully, represent the dominant physical processes. Following Galitskii,[11] we argue that, in the low-density regime for a system with short-range interactions, the leading contribution comes from graphs with the smallest number of internal hole lines, i.e., the ladder diagrams. This follows from the Fermi factor $f=\{\exp[\beta(\varepsilon_{\mathbf{k}}-\mu)]+1\}^{-1}$ associated with each hole propagator as compared to the factors of $1-f$ for particle propagators. This approximation focuses on the repeated scattering of two particles, or two holes, and ignores, for example, density fluctuations in the particle-hole channel.

The vertex part Γ in the particle-particle channel, within the ladder approximation (see Fig. 1), is given by

$$\tilde{\Gamma}_{\mathbf{k},\mathbf{k}'}(\mathbf{q},i\omega_\nu)=V_{\mathbf{k},\mathbf{k}'}+\sum_{\mathbf{p},\mathbf{p}'}V_{\mathbf{k},\mathbf{p}}\tilde{\mathcal{H}}_{\mathbf{p},\mathbf{p}'}(\mathbf{q},i\omega_\nu)\tilde{\Gamma}_{\mathbf{p}',\mathbf{k}'}(\mathbf{q},i\omega_\nu)\ , \tag{9}$$

where $i\omega_\nu=2\nu\pi i/\beta$ is a Bose Matsubara frequency. The kernel, which represents the propagation of two fermions in the medium, is given by

$$\begin{aligned}\tilde{\mathcal{H}}_{\mathbf{p},\mathbf{p}'}(\mathbf{q},i\omega_\nu)&=-\frac{1}{\beta}\sum_{ip_n}\frac{1}{ip_n-\varepsilon_{\mathbf{p}+\mathbf{q}/2}+\mu}\\&\quad\times\frac{1}{i\omega_\nu-ip_n-\varepsilon_{-\mathbf{p}+\mathbf{q}/2}+\mu}\delta_{\mathbf{p},\mathbf{p}'}\\&=\frac{1-f(\varepsilon_{\mathbf{p}+\mathbf{q}/2}-\mu)-f(\varepsilon_{-\mathbf{p}+\mathbf{q}/2}-\mu)}{i\omega_\nu-\varepsilon_{\mathbf{p}+\mathbf{q}/2}-\varepsilon_{-\mathbf{p}+\mathbf{q}/2}+2\mu}\delta_{\mathbf{p},\mathbf{p}'}\ ,\end{aligned} \tag{10}$$

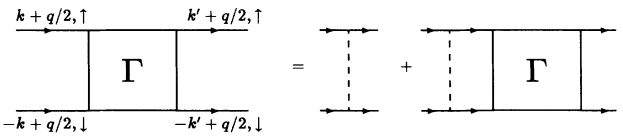

FIG. 1. Ladder approximation for the vertex part Γ describing the scattering of two fermions in the medium. The fermions have opposite spin, relative momentum $2\hbar\mathbf{k}$, and center-of-mass momentum $\hbar\mathbf{q}$.

where the internal frequencies are fermionic, $ip_n=(2n+1)\pi i/\beta$. The retarded vertex part $\Gamma(\mathbf{q},\omega)$ is given, as usual, by the analytic continuation $\Gamma(\mathbf{q},\omega)\equiv\tilde{\Gamma}(\mathbf{q},\omega+i\eta)$.

It is now convenient to eliminate the interaction potential in (9), and express it in terms of the two-body T matrix of (8) for the reasons discussed before. We thus obtain

$$\tilde{\Gamma}_{\mathbf{k},\mathbf{k}'}(\mathbf{q},i\omega_\nu)=T_{\mathbf{k},\mathbf{k}'}(\mathbf{q}',\omega')+\sum_{\mathbf{p},\mathbf{p}'}T_{\mathbf{k},\mathbf{p}}(\mathbf{q}',\omega')[\tilde{\mathcal{K}}_{\mathbf{p},\mathbf{p}'}(\mathbf{q},i\omega_\nu)-\mathcal{K}^0_{\mathbf{p},\mathbf{p}'}(\mathbf{q}',\omega')]\tilde{\Gamma}_{\mathbf{p}',\mathbf{k}'}(\mathbf{q},i\omega_\nu)\ . \tag{11}$$

Here we are free to choose the arguments $(\mathbf{q},i\omega_\nu)$ and $(\mathbf{q}',\omega')$ independently, since the interaction V does not depend on any of these variables.

In the low-energy regime relevant to the dilute limit, T is independent of the momentum labels, from which it follows that $\tilde{\Gamma}$ is also separable. Consequently, for $kR\ll 1$ and $k'R\ll 1$, (11) reduces to a scalar equation and can be easily solved to give

$$\tilde{\Gamma}_{\mathbf{k},\mathbf{k}'}(\mathbf{q},i\omega_\nu)\approx\tilde{\Gamma}(\mathbf{q},i\omega_\nu)=\frac{1}{\tau_0^{-1}(\mathbf{q}',\omega')+\chi^0(\mathbf{q}',\omega')-\tilde{\chi}(\mathbf{q},i\omega_\nu)}\ , \tag{12}$$

where

$$\tilde{\chi}(\mathbf{q},i\omega_\nu)=\sum_{\mathbf{k}}\tilde{\mathcal{K}}_{\mathbf{k}\mathbf{k}}(\mathbf{q},i\omega_\nu) \tag{13}$$

and

$$\chi^0(\mathbf{q},\omega)=\sum_{\mathbf{k}}\mathcal{K}^0_{\mathbf{k}\mathbf{k}}(\mathbf{q},\omega)\ . \tag{14}$$

The result (12) for the vertex part is independent of the primed variables on the right-hand side. We can thus choose $\mathbf{q}'=\mathbf{0}$, and use the results for the two-body problem obtained earlier. The ultraviolet divergence of $\tilde{\chi}$, arising from the integration in (13), is canceled by the identical one from χ^0 in (14). The infrared divergence in τ_0^{-1} is canceled by a similar divergence in χ^0 as discussed below.

C. Expansion parameter

The logarithm in $\tau_0^{-1}(\omega')$ in (12) is effectively cutoff on the scale of $2\varepsilon_F$ which is the natural scale for two-particle energies in the many-body system. Consequently, the scattering amplitude on the Fermi surface, $\mathrm{Re}[\tau_0(2\varepsilon_F)]$, emerges as the small parameter in the problem, which we define as

$$g\equiv\frac{1}{\ln(E_a/2\varepsilon_F)}\ll 1\ . \tag{15}$$

Our solution (12), which is of the form $\tilde{\Gamma}=1/(1/g-X)$, differs from that of the usual Galitskii[11] analysis in 3D and its 2D extension by Bloom[21] in that it includes contributions to all orders in the scattering amplitude g. The Galitskii-Bloom results can be obtained by expanding the above expression to second order in g, i.e., $\tilde{\Gamma}\simeq g+g^2X$. While no new physics is obtained in the low-density limit in 3D by going beyond $O(g^2)$, this is not so in 2D as we shall see in the following sections.

It should be stressed that, for a general potential, (12) is exact only to second order. Beyond that it sums an infinite class of diagrams but makes an approximation in that (a) it ignores the higher ($l>0$) angular momentum scattering channels, (b) it accounts for only two-body collisions, and (c) it ignores any polarization of the medium. The second point is important in that, even if one defines the problem to have only s-wave interactions, the neglect of three- and higher-body collisions makes a systematic low-density expansion to higher orders difficult.[12] In spite of this caveat, we will see below that it is essential for our purposes to go to all orders in g, since the bound states we will find below have as essential singularity $\exp(-1/g)$ and thus cannot be obtained in any finite order of perturbation theory.

We conclude this section with a discussion of the region of validity of the low-density expansion in 2D. To understand the inequality (15), we return to the example of the repulsive disk potential: $V(r)=V_0\Theta(R-r)$ with the parameter E_a given by Eq. (6). The low-density regime requires $\varepsilon_F\ll\varepsilon_R=\hbar^2/2mR^2$. For weak repulsion $V_0\ll\varepsilon_R/\ln(\varepsilon_R/\varepsilon_F)$, we have $g\simeq V_0/\varepsilon_R$, and the expansion parameter is essentially the potential strength.

In the more interesting limit of a hard-core potential ($V_0\to\infty$), the expansion parameter is $g\simeq 1/\ln(\varepsilon_R/\varepsilon_F)$. The requirement $1/\ln(1/k_FR)\ll 1$ is much more stringent than merely $k_FR\ll 1$. Thus, as the potential strength increases, the regime of densities in which the results are valid become more restrictive.

Finally, one can make contact with the low-density limit of the Hubbard model by replacing the "range" R by the lattice spacing a, V_0 by U, and ε_R by t, the hopping energy. Using $\varepsilon_F=\pi\hbar^2n/m=2\pi tna^2$, where n is the density, we can obtain from (6) and (15) the expansion parameter in 2D. For weak coupling this is just U/t, however, for $U/t\gg 1$, the regime of validity is given by

$$g_{\text{Hubbard}}=1/\ln(1/na^2)\ll 1\ . \tag{16}$$

III. BOUND STATES

Having obtained the vertex part in the particle-particle channel in the previous section, we now turn to an analysis of its singularities as a function of the energy variable ω, for fixed q. A branch cut in the vertex part represents a continuum of two-particle scattering states, while an isolated pole is associated with a collective mode, or a bound state. Since we are dealing with a normal (i.e., nonsuperfluid) system, one would not expect a bound state in the particle-particle channel. However, we will find that, in two dimensions, such a mode does exist for $q<2k_F$, and disperses down linearly to zero at

$q=2k_F$. We will first show the existence of this pole pictorially (for all temperatures), and then obtain an analytical form for its $T=0$ dispersion.

Mathematically, the new bound state is analogous to collective modes like zero sound or plasmons which are isolated poles in the particle-hole channel vertex part separated from the particle-hole continuum. However, what makes the new poles unusual is that they are in the particle-particle channel. For attractive interactions one is familiar with particle-particle channel poles, in the upper half plane, which signal the superconducting instability. In our case, the interactions are repulsive, the poles are on the real axis, and there is no associated instability. We will argue that the bound-state poles represent well-defined excitations of the system.

A. Graphical analysis of the pole structure of Γ

In this subsection we will work in a finite $L\times L$ box, so that all singularities of the vertex part of (12), including possible branch cuts, will appear as discrete poles. We thus seek solutions z, for fixed $\mathbf{q}$, to the equation $\tilde{\Gamma}^{-1}(\mathbf{q},z)=0$, where we have made the analytic continuation $i\omega_\nu\rightarrow z$.

The fact that the rhs of (12) is independent of $(\mathbf{q}',\omega')$ can be exploited by choosing convenient values for these variables, such as $\mathbf{q}'=\mathbf{0}$ and $\omega'=-2\mu<0$. Using the T-matrix of (8), with g defined in (15), we can rewrite (12) as

$$\frac{1}{C\tilde{\Gamma}(\mathbf{q},z)}=\frac{1}{g}+\frac{1}{C}\sum_{\mathbf{k}}\left[-\tilde{\mathcal{K}}_{\mathbf{kk}}(\mathbf{q},z)-\frac{1}{2\varepsilon_{\mathbf{k}}+2\mu}\right], \tag{17}$$

where $C=mL^2/4\pi\hbar^2$, which is related to the density of states through $C=(1/4)L^2\,dn/d\varepsilon$. We have also used $\mu=\varepsilon_F$, thus ignoring the shift in energies due to the interaction which is higher order in g.

Using (10) and the identities $\frac{1}{2}-f(x)=\frac{1}{2}\tanh(\beta x/2)$ and

$$\tanh(a+b)+\tanh(a-b)$$
$$=2\tanh(2a)[1+\cosh(2b)/\cosh(2a)]^{-1},$$

in the above equation, we find that the poles of $\Gamma(\mathbf{q},z)$ are determined by

$$\frac{-1}{g}=\frac{1}{2C}\sum_{\mathbf{k}}\left[\frac{\tanh[\beta(\varepsilon_{\mathbf{k}}+\varepsilon_{\mathbf{q}/2}-\mu)/2]}{\varepsilon_{\mathbf{k}}+\varepsilon_{\mathbf{q}/2}-\mu-z/2}F(k,q,\phi)-\frac{1}{\varepsilon_{\mathbf{k}}+\mu}\right], \tag{18}$$

where

$$F(k,q,\phi)=\{1+\cosh(2\beta\sqrt{\varepsilon_{\mathbf{k}}\varepsilon_{\mathbf{q}/2}}\cos\phi)/\cosh[\beta(\varepsilon_{\mathbf{k}}+\varepsilon_{\mathbf{q}/2}-\mu)]\}^{-1} \tag{19}$$

with ϕ the angle between $\mathbf{k}$ and $\mathbf{q}$.

Consider first the *noninteracting* case: $g=0$. The free two-particle propagator clearly has poles at

$$z=\omega_{\text{free}}(\mathbf{k},\mathbf{q})=\varepsilon_{\mathbf{k}+\mathbf{q}/2}+\varepsilon_{-\mathbf{k}+\mathbf{q}/2}-2\mu\ .$$

These solutions are simply products of two single-particle plane waves with relative momentum $2\hbar\mathbf{k}$ and center-of-mass momentum $\hbar\mathbf{q}$. For any given $\mathbf{q}$, the allowed values of $\mathbf{k}$ become dense in an infinite system. One then obtains a branch cut, representing the band of incoherent two-particle scattering states. For each $\mathbf{q}$, the bottom of the two-particle band is at frequency ω_q^* given by

$$\omega_q^*\equiv\min_k(\varepsilon_{\mathbf{k}+\mathbf{q}/2}+\varepsilon_{-\mathbf{k}+\mathbf{q}/2}-2\mu)$$
$$=\hbar^2q^2/4m-2\mu=2(\varepsilon_{q/2}-\mu)\ . \tag{20}$$

Let us now see how interactions modify the two-particle spectrum. We focus only on the real z axis and, in the remainder of this subsection, use $\omega=\text{Re}\{z\}$. We look for the poles of the vertex part by graphical solution of (18) as shown in Fig. 2. The solutions of (18) are given by the intersection of the solid curve, representing the rhs as a function of ω, with the horizontal dashed line at $-1/g$. The vertical dashed lines indicate the noninteracting solutions.

For $q>2k_F$, the argument of the tanh function in (18) is always positive. A graphical solution (analogous to the one shown in Fig. 2 for the case of $q<2k_F$) shows that the poles of the vertex part in the interacting system are sandwiched between those of the noninteracting system

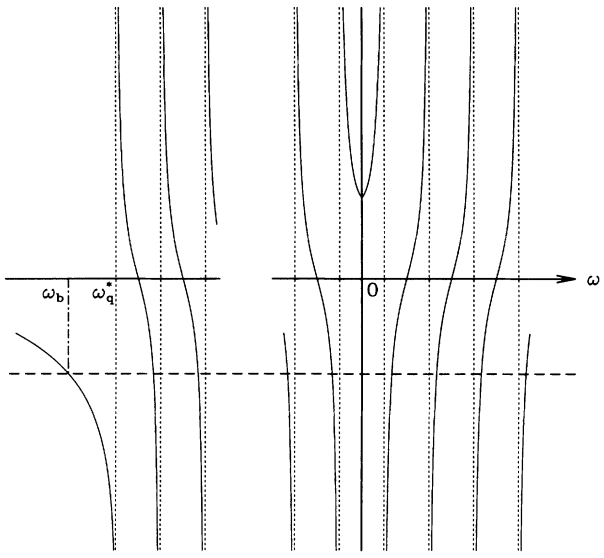

FIG. 2. Poles of the vertex part Γ representing the two-particle spectrum in a finite box are obtained by a graphical solution of Eq. (18) for fixed $\mathbf{q}$. For repulsive interactions $-g^{-1}$ (shown as the horizontal dashed line) intersects the left-hand side of Eq. (18) (the solid curves), plotted as a function of $\omega=\text{Re}z$, at a series of closely spaced points within the two-particle band $\omega\geq\omega_q^*$. These form a branch cut in the infinite volume limit. In addition, for $q<2k_F$, there is an isolated pole at $\omega_b(q)$ below the bottom of the band ω_q^* in 2D.

at $\omega_{\text{free}}(\mathbf{k},\mathbf{q})$. In the infinite volume limit these closely spaced poles, with interlacing zeros, merge to form a branch cut. For $q>2k_F$, the singularity structure of the vertex part is thus the same as for the noninteracting system: a branch cut on the real axis for $\omega>\omega_q^*>0$.

For $q<2k_F$, the argument of the tanh can change sign leading to the change in slope of the solid curve at $\omega=0$ as shown in Fig. 2. (The curve plotted in this figure is well known from superconductivity; the pairing instability is related to the disappearance of two poles from the real axis, for the case of an attractive interaction $g<0$, which is evident from looking at positive values of the ordinate.) Here we are interested in repulsive interactions for which the lhs of (18) is negative, and thus we focus on negative values of the ordinate. We immediately see a new feature: in addition to the incoherent scattering states there is a new solution $\omega=\omega_b(q)$, split off below the two-particle band $[\omega_b(q)<\omega_q^*]$, which did not exist in the noninteracting system. The two-particle spectrum is shown in Fig. 3.

It might seem that a similar graphical analysis of the *three-dimensional* case would also yield such a solution. This is not true since the existence of this solution requires a nonzero density of states near $\mathbf{k}=0$, which is the bottom of the band *in the relative coordinate*. Such a nonvanishing density of states is available in two dimensions, but not in three. The importance of two-dimensionality will be further clarified by the analytical calculation in the following subsection.

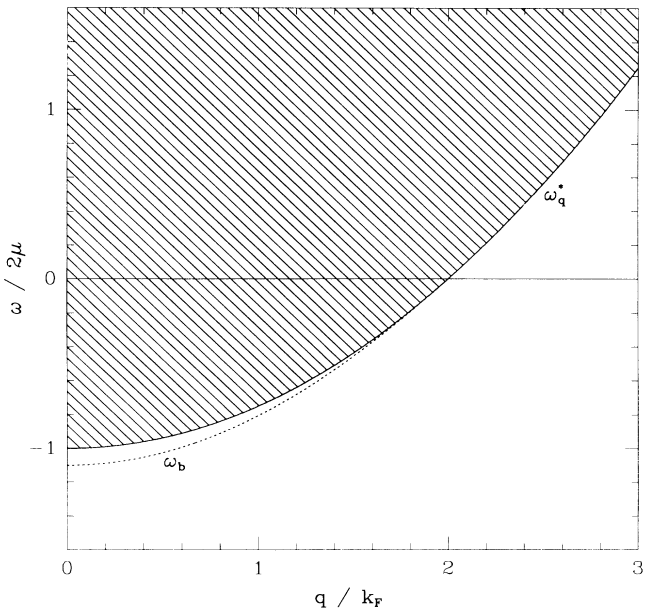

FIG. 3. The particle-particle channel spectrum plotted as a function of the center-of-mass momentum q. For each $\mathbf{q}$ there is a continuum of states, $\omega(\mathbf{q},\mathbf{k})=\varepsilon_{\mathbf{k}+\mathbf{q}/2}+\varepsilon_{-\mathbf{k}+\mathbf{q}/2}-2\mu$, starting at the bottom of the two-particle band at ω_q^*, and labeled by increasing values of the relative momentum $2\mathbf{k}$. In addition, for each $q<2k_F$, there is an isolated state below the band at $\omega_b(q)$. The separation $|\omega_q^*-\omega_b(q)|$ has been somewhat exaggerated for clarity.

B. Dispersion

To determine the dispersion for the collective mode, and to understand its effects upon various physical quantities in later sections, we work at $T=0$. This allows us to obtain analytical results in many cases. We will be interested in the retarded vertex function Γ^{-1}, which is obtained from $\tilde{\Gamma}^{-1}$ by the usual analytic continuation:

$$\Gamma^{-1}(\mathbf{q},\omega)=\tilde{\Gamma}^{-1}(\mathbf{q},\omega+i\eta)$$
$$=C[A(\mathbf{q},\omega)+iB(\mathbf{q},\omega)]\ , \tag{21}$$

where $A(\mathbf{q},\omega)$ and $B(\mathbf{q},\omega)$ are the real and imaginary parts of Γ^{-1} with a factor of $C=mL^2/4\pi\hbar^2$ taken out for later convenience. Once the thermodynamic limit is taken, the roots of (21) only give the isolated poles. Using $(x\pm i\eta)^{-1}\to\mathcal{P}x^{-1}\mp i\pi\delta(x)$, where $\mathcal{P}$ indicates the principal value, we see that the continuum of scattering states are now accounted for by the nonzero value of $B(\mathbf{q},\omega)$ within the two-particle band $\omega>\omega_q^*$.

The energy of the bound state is obtained by solving $A(\mathbf{q},\omega_b(q))=0$. We expect from the preceding analysis that $\omega_b(q)<\omega_q^*$ and therefore $B\equiv 0$, which can also be seen by inspection of the retarded version of (17). For convenience we scale all two-particle energies with 2μ and introduce the dimensionless variables

$$\tilde{\omega}=\omega/2\mu\ ,$$
$$u_q=\omega_q^*/2\mu\ . \tag{22}$$

To make further progress, we need a simple expression for $A(\mathbf{q},\omega)$ for $\omega<\omega_q^*$, i.e., below the bottom of the band. Towards this end, we make the transformation $\mathbf{k}\to\mathbf{k}\mp\mathbf{q}/2$ in the two terms with the Fermi functions [see (10)] in the kernel of (17). Writing the contribution of these two terms in dimensionless variables we get

$$-\int_0^\infty dx\int_0^{2\pi}\frac{d\phi}{2\pi}f(\mu(x-1))$$
$$\times\left[\frac{1}{a-b\cos\phi}+\frac{1}{a+b\cos\phi}\right] \tag{23}$$

with $a=x+2u_q+1-\tilde{\omega}$ and $b=2\sqrt{x(u_q+1)}$, where $x=\varepsilon_{\mathbf{k}}/\mu$. We next use the identity

$$\int_0^\pi d\phi(a+b\cos\phi)^{-1}=\pi\,\mathrm{sgn}(a)\Theta(a^2-b^2)/\sqrt{a^2-b^2}$$

to perform the angular integration. Now

$$a^2-b^2=x^2-2(\tilde{\omega}+1)x+(2u_q+1-\tilde{\omega})^2>0$$

for all x. The last inequality follows from the fact that the roots $x_\pm=\tilde{\omega}+1\pm 2\sqrt{(\tilde{\omega}-u_q)(u_q+1)}$ of a^2-b^2 are complex since $\tilde{\omega}<u_q$. Thus, at $T=0$, we may rewrite (23) as

$$-2\int_0^1 dx\frac{1}{\sqrt{a^2-b^2}}$$
$$=-2\ln\left[\frac{\sqrt{1-2(\tilde{\omega}+1)+(2u_q+1-\tilde{\omega})^2}-\tilde{\omega}}{2(u_q-\tilde{\omega})}\right]\ . \tag{24}$$

The remaining terms in (17) can easily be evaluated using

$$\mathcal{P}\int_0^\infty dx\left[\frac{1}{x+u_q-\tilde{\omega}}-\frac{1}{x+1}\right]=\ln\frac{1}{u_q-\tilde{\omega}}\ . \tag{25}$$

Putting all this together, we then get the following expression which is valid below the bottom of the band:

$$A(\mathbf{q},\omega)=\frac{1}{g}+\ln[u_q-\tilde{\omega}] -2\ln[\sqrt{(u_q+1)(u_q-\tilde{\omega})+\tilde{\omega}^2/4}-\tilde{\omega}/2]\ . \tag{26}$$

To solve for $A(\mathbf{q},\omega)=0$, one simply expands the square root in the small quantity $u_q-\tilde{\omega}$, which specifies how far below the bottom of the band the isolated pole is. The leading contribution expressed in terms of the original variables is

$$A(\mathbf{q},\omega)\approx\frac{1}{g}+\ln[2\mu(\omega_q^*-\omega)/(\omega_q^*)^2]\ , \tag{27}$$

which is valid for $q<2k_F$, or equivalently $\omega_q^*<0$. From the root of this equation we find the collective mode frequency

$$\omega_b(q)=\omega_q^*-\exp(-1/g)(\omega_q^*)^2/2\mu,\quad q<2k_F\ . \tag{28}$$

There is no solution for $q>2k_F$, as expected from the graphical analysis. The expression for $\omega_b(q)$ above has an essential singularity in g.

The existence of this pole can be traced back to the propagation of two holes associated with the second term in $(1-f_+)(1-f_-)-f_+f_-$ leading to the numerator in (10). It is also clear that this state is collective in that it requires a Fermi sea for its existence, i.e., it does not exist for the two-body problem where $k_F=0$.

The energy of a hole state is measured from the Fermi surface downwards, so that its energy increases as one goes farther below $\omega=0$. The bound state associated with each isolated pole then has *positive excitation energy* $|\omega_b(q)|$, even though the pole frequencies lie below the bottom of the band of two-particle states associated with each $\mathbf{q}$. The energy dispersion of the bound state is then

$$\omega=|\omega_b(q)|\ , \tag{29}$$

which vanishes linearly at $q=2k_F$ and attains a maximum at $q=0$. We thus obtain, from the particle-particle channel spectrum of Fig. 3, the excitation spectra for two holes and for two particles shown in Fig. 4. Our interpretation of the bound state as a bound excitation of a pair of holes will be further clarified when we consider its effect on the thermodynamics of the system in Sec. V below.

Even though the two-particle excitation spectrum is not bounded above, a finite density implies that the two-hole excitations do have an upper band edge for each $q<2k_F$, and the poles we have found may be thought of as antibound states of holes. A crucial property of the 2D gas which leads to these bound excitations is the nonvanishing density of states at small momenta.

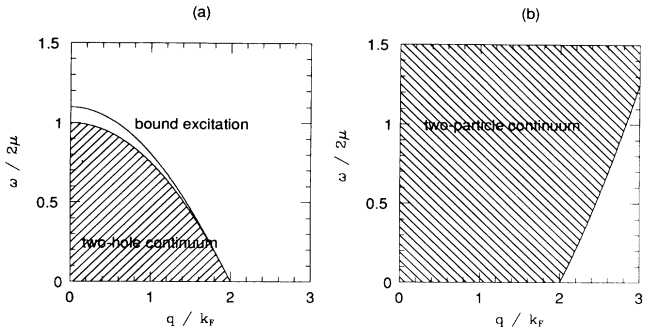

FIG. 4. (a) The spectrum of two-hole excitations including the bound excitations, with dispersion $\omega=|\omega_b(q)|$ for $q<2k_F$, which lie above the band. This spectrum is obtained simply by taking the absolute value of the negative frequency spectrum in Fig. 3. (b) Spectrum of two-particle excitations.

Specifically, it is density of states associated with the scattering of fermions with zero relative momentum, i.e., $|\mathbf{p}\uparrow\rangle$ and $|\mathbf{p}\downarrow\rangle$ which is responsible for this effect. The low-lying bound hole excitations then involve momenta $\mathbf{p}$ close to the Fermi surface.

In the discussion on the expansion parameter it was pointed out that g in (28) is small for arbitrary weak or strong repulsion, provided that the appropriate diluteness criterion is met. It should, however, be noted that, even though our results apply to the hard-disk limit, the low-density restriction leads to a "weak-coupling expansion" since one perturbs about plane-wave states. Also, in analogy with the thresholds for (attractive) Cooper pairing in 2D and 3D, one might ask whether similar bound hole excitations might appear in 3D above some threshold repulsion. Apart from the density-of-states considerations, this inherently weak-coupling nature of the dilute-gas expansion precludes any such states in 3D for the low-density systems we consider.

IV. PHASE-SHIFT ANALYSIS

We investigate the effect of this bound state on various physical quantities in order to develop some understanding of its nature. In this section we look at the phase shift $\delta(\mathbf{q},\omega)$, which characterizes two-particle scattering in the dilute Fermi system, and is defined by

$$\Gamma(\mathbf{q},\omega)=|\Gamma|\exp[i\delta(\mathbf{q},\omega)]\ . \tag{30}$$

$\delta(\mathbf{q},\omega)$ is the many-body analogue of the more familiar phase shift which describes the scattering of particles off a potential. This analogy is explored further in the Appendix, where we also establish a connection—Levinson's theorem—between the phase shift at the bottom of the band and the bound states.

There are at least two good reasons to study the phase shift. First, we will show in the following section [see Eq. (47)] that the thermodynamics of the interacting many-body system is very simply related to $\delta(\mathbf{q},\omega)$. Second, it has been suggested in the recent literature[7,8] that a nonzero Fermi-surface phase shift $\delta(2k_F,0)$ signals a breakdown of Fermi-liquid theory. We find that $\delta(2k_F,\omega\to0)=0$, but further argue that this value can-

not be used as a diagnostic for the Fermi-liquid theory (see Sec. VI).

A. Further analysis of the vertex part

We have earlier obtained a simple expression for $A(\mathbf{q},\omega)$, namely, (26), which was valid below the bottom of the band, where $B\equiv 0$. We now need to obtain more general expressions[22] for $A(\mathbf{q},\omega)$ and $B(\mathbf{q},\omega)$, which are valid for all q and ω. We begin with the retarded form of (12) at zero temperature. We use the T matrix of (8) and choose $\mathbf{q}'=0$ and $\omega'=-|\omega-\omega_q^*|$ [instead of $\omega'=-\mu$ used in (17)]. Using the dimensionless variables introduced in (22) and defining $\Delta\omega=\omega-\omega_q^*$, we get

$$\frac{1}{C\Gamma(\mathbf{q},\omega)}\equiv A+iB$$
$$=\frac{1}{g}+\ln\left[\frac{1}{|\Delta\tilde{\omega}|}\right]+\int_0^\infty dx\int_0^\pi\frac{d\phi}{\pi}\left[\frac{h(x,u_q,\phi)}{x-\Delta\tilde{\omega}-i\eta}-\frac{1}{x+|\Delta\tilde{\omega}|}\right] \tag{31}$$

with the occupation factor

$$h(y,z,\phi)=1-2\Theta[-y-z-2\sqrt{y(z+1)}\cos\phi]\ .$$

The angular integral is given by

$$\int_0^\pi\frac{d\phi}{\pi}h(x,u_q,\phi)=\begin{cases}\mathrm{sgn}(q-2k_F) & \text{for } \xi_-(q)>x+u_q\\ 1-F(x+u_q,u_q) & \text{for } \xi_+(q)>x+u_q>\xi_-(q)\\ 1 & \text{for } x+u_q>\xi_+(q)\ ,\end{cases} \tag{32}$$

where

$$\xi_\pm(q)=2(u_q+1\pm\sqrt{u_q+1}) \tag{33}$$

and

$$F(y,u_q)\equiv\frac{2}{\pi}\arccos\left[\frac{y}{2\sqrt{(y-u_q)(u_q+1)}}\right]\ . \tag{34}$$

We thus find that the real imaginary parts of (31) are given by[22]

$$A(\mathbf{q},\omega)=\frac{1}{g}+\ln\left[\frac{|\tilde{\omega}-u_q|}{[\xi_-(q)-\tilde{\omega}]^2}\right]-\int_{\xi_-(q)}^{\xi_+(q)}\frac{dy}{(y-\tilde{\omega})}F(y,u_q)\quad\text{for } q<2k_F\ , \tag{35}$$

while

$$A(\mathbf{q},\omega)=\frac{1}{g}-\ln|\tilde{\omega}-u_q|-\int_{\xi_-(q)}^{\xi_+(q)}\frac{dy}{(y-\tilde{\omega})}F(y,u_q)\quad\text{for } q>2k_F \tag{36}$$

and

$$B(\mathbf{q},\omega)=\pi\Theta(\tilde{\omega}-u_q)\times\begin{cases}\mathrm{sgn}(q-2k_F) & \text{for } \tilde{\omega}<\xi_-(q)\\ 1-F(\tilde{\omega};u_q) & \text{for } \xi_-(q)<\tilde{\omega}<\xi_+(q)\\ 1 & \text{for } \xi_+(q)<\tilde{\omega}\ .\end{cases} \tag{37}$$

The integral in (35) has to be evaluated numerically for most values of the center-of-mass momentum. However, these expressions make explicit the locations of various features in the phase shift, as will be apparent below, and will also prove useful for making asymptotic expansions.

B. Phase shifts

We are now in a position to explicitly compute the two-particle phase shift $\delta(\mathbf{q},\omega)$ for the many-body system. From (30) we see that the phase shift is only defined modulo 2π and requires the additional prescription that $\delta\to 0$ as $\omega\to\pm\infty$. Levinson's theorem proved in the Appendix states that

$$\delta(q,\omega_q^*)=n_q\pi\ , \tag{38}$$

where n_q is the number of bound states below the two-particle band. In the preceding sections, we found that $n_q=\Theta(2k_F-q)$ and thus the phase shift is confined to the range $(-\pi,\pi)$]. The phase shift is then given by

$$\delta(\mathbf{q},\omega)=\arctan[-B(\mathbf{q},\omega)/A(\mathbf{q},\omega)] \tag{39}$$

subject to the above considerations.

The phase shift can now be found from the above equation with A and B given by (35) and (37). In brief, the results are as follows. The presence of the bound-state pole, for $q<2k_F$, leads to a discontinuous jump in the phase shift from zero to π as ω increases through the bound-state energy $\omega_b(q)$. As ω increases further, the phase shift remains at π until the bottom of the band ω_q^*.

Within the band, δ decreases monotonically from π to zero at the Fermi surface $\omega=0$, and then takes on negative values for $\omega>0$.

We now turn to a discussion of the numerical results and the asymptotic forms. For all the figures in this section, we have taken the value of $E_a=200\mu$, or equivalently $g=1/\ln(100)\simeq 0.217$, for the parameter characterizing the interaction.

For $q=0$, one has $\xi_+(0)=\xi_-(0)=0$, and the integral in (35) may be evaluated analytically to obtain

$$A(0,\omega)+iB(0,\omega)=\frac{1}{g}+\ln\left[\frac{2\mu|\omega+2\mu|}{\omega^2}\right]+i\pi\Theta(\omega+2\mu)\mathrm{sgn}(\omega)\ . \quad (40)$$

The phase shift $\delta(0,\omega)$ from this is plotted as a function of ω in Fig. 5. As described in the summary above, δ jumps from 0 to π as ω increases through $\omega_b(0)$, reflecting the existence of the bound state. In 2D, the initial decrease in δ just above the bottom of the band follows the logarithmically singular form

$$\delta(q,\omega)\to\pi\left[1+\frac{1}{1/g+\ln\{|\tilde{\omega}-u_q|/[u_q-\xi_-(q)]^2\}}\right] \quad \text{as } \tilde{\omega}\to u_q^+ \text{ for } q\neq 2k_F \quad (41)$$

as can be verified from (35) and (37).

After the sharp falloff, the phase shift decreases monotonically within the band, with another singular feature at the Fermi surface. At $\omega=0$ the phase shift goes through zero logarithmically with

$$\delta(0,\omega)\to\frac{-\pi\,\mathrm{sgn}(\tilde{\omega})}{1/g+\ln(1/\tilde{\omega}^2)} \quad \text{as } \tilde{\omega}\to 0\ , \quad (42)$$

which follows from (40). As ω increases through the Fermi surface it becomes negative and flattens off again. The singularity in (42) is not special to 2D and comes from the discontinuity in the occupation factors in (13) at the Fermi surface which exists in all dimensions.[23]

It is worth commenting on the sign of the phase shift. In ordinary potential scattering theory $\delta<0$ signifies a repulsive interaction (see the Appendix). From this point of view the sign change in δ at the Fermi surface $\omega=0$ may appear puzzling. However, we will find that the positive phase shift below the Fermi surface will lead to an increase in energy, characteristic of repulsive interactions, since, in the free energy in (47), the Bose factor $g(\omega)$ multiplying the phase shift also changes sign at $\omega=0$.

For $0<q<2k_F$, the phase shift has to be obtained numerically. In Fig. 6 the solid curve represents the results of such a calculation for $q=0.5k_F$. The structure near the bottom of the band $u_{k_F/2}=-0.9375$ is qualitatively similar to the previous case. The new features, different from the $q=0$ case, are (i) the shoulders at $\tilde{\omega}=\xi_\pm(q)$, and (ii) the linear vanishing of the phase shift at the Fermi surface. This can be seen analytically by using the asymptotic forms valid for $0<q<2k_F$. We find

$$A(\mathbf{q},\omega)\to\frac{1}{g}+\ln|u_q|/\xi_-(q)^2-\int_{\xi_-(q)}^{\xi_+(q)}\frac{dy}{y}F(y,u_q) \quad \text{as } \tilde{\omega}\to 0 \quad (43)$$

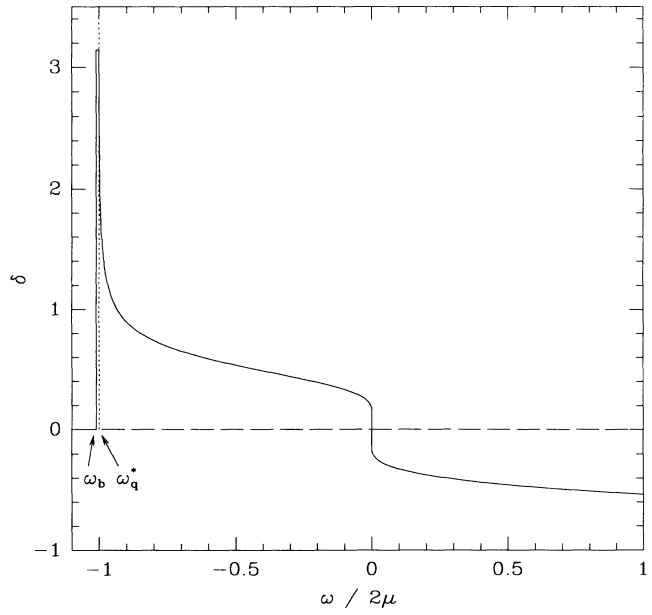

FIG. 5. Phase shift as a function of ω for fixed $q=0$ (i.e., $u_q=-1$, and $\xi_-=\xi^+=0$) from Eq. (40) for the parameter $g=1/\ln(100)$. As δ increases through $\omega_b(q)$, it jumps from zero to π; it remains at π until the bottom of the band ω_q^* after which it drops off very rapidly, then flattens off and finally again decreases logarithmically through zero at the Fermi surface $\omega=0$.

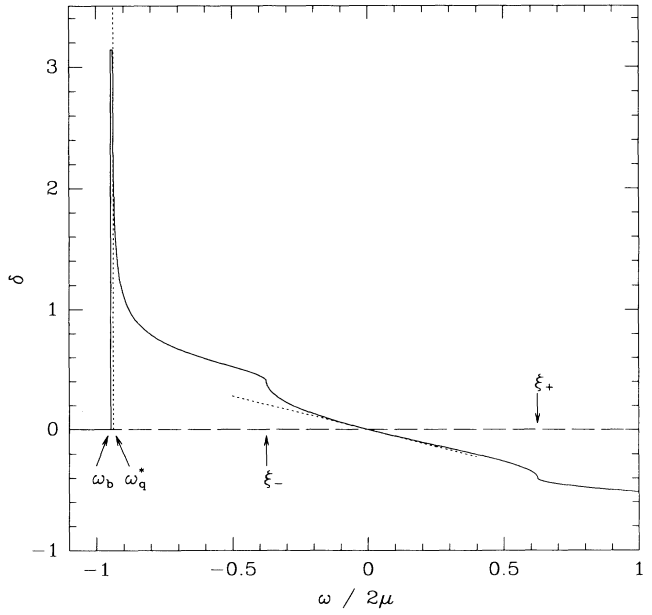

FIG. 6. Phase shift as a function of ω for fixed $q=0.5k_F$ (i.e., $u_q=-0.9375$, $\xi_-=0.375$, and $\xi_+=0.625$) calculated numerically for $g=1/\ln(100)$. The new features compared with those shown in Fig. 5 are the cusps at $\xi_-(q)$ and $\xi_+(q)$, and the linear decrease of δ through zero at the Fermi surface—indicated by the dotted line.

and

$$B(\mathbf{q},\omega)\to\tilde{\omega}/\sqrt{|u_q|(u_q+1)} \quad \text{as } \tilde{\omega}\to 0 \tag{44}$$

on expanding the arccosine. It then follows that

$$\delta(0<q<2k_F,\omega)\to -gK(q)\tilde{\omega} \quad \text{as } \tilde{\omega}\to 0\ , \tag{45}$$

where the coefficient $K(q)$ can be calculated. This asymptotic form is plotted as the dotted curve in Fig. 6.

For $q=2k_F$, the bottom of the band as well as $\xi_-(2k_F)$ coincides with the Fermi surface. There is then no bound-state pole, the phase shift is zero for $\omega\le 0$, and there is no logarithmic decrease just above the bottom of the band as in (41). The numerically evaluated phase shift is shown as the solid curve in Fig. 7. By integrating (35) by parts, one can show that, for small frequencies, $A(2k_F,\omega)\to 1/g+$ smaller terms, while $B(2k_F,\omega)\to\sqrt{\tilde{\omega}}\Theta(\tilde{\omega})$ to give the asymptotic phase shift

$$\delta(2k_F,\omega)\to -g\sqrt{\tilde{\omega}}\Theta(\tilde{\omega}) \quad \text{as } \tilde{\omega}\to 0 \tag{46}$$

near the Fermi surface, which we plot as the dotted curve in Fig. 7.

For the case of $q>2k_F$, the phase shift is zero for all frequencies below the bottom of the band u_q, which is now positive. In Fig. 8, the solid line shows the numerically calculated phase shift for $u_q=0.01$, i.e., for $q=2\sqrt{1.01}k_F$. The phase shift again drops off logarithmically above ω_q^* as in (41) but now increases rapidly above $\xi_-(q)$ (which is now very close to ω_q^*) leading to a sharp spike. It then decreases again to a shoulder feature at $\xi_+(q)$. The detailed form of the spike is shown in the

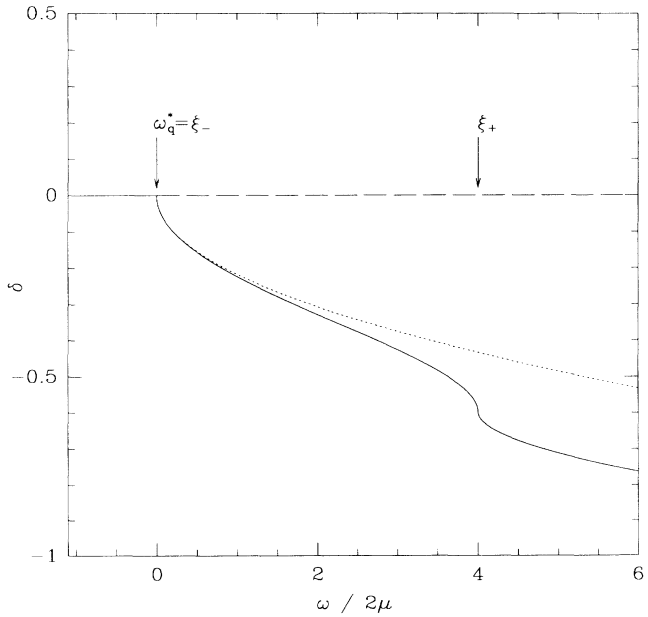

FIG. 7. Phase shift as a function of ω for fixed $q=2k_F$ (i.e., $u_q=\xi_-=0$ and $\xi_+=4$) calculated numerically for $g=1/\ln(100)$. For this special case, $\xi_-(q)$ coincides with the bottom of the band ω_q^* as well as the Fermi surface $\omega=0$. Here the initial decrease in δ follows the $\sqrt{\omega}$ asymptotic form of Eq. (46), indicated by the dotted line, rather than the more rapid logarithmic decrease for the other cases.

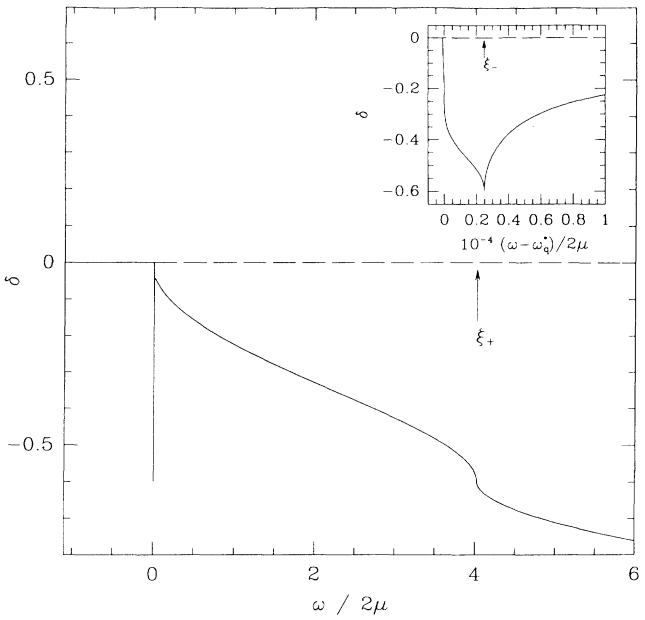

FIG. 8. Phase shift as a function of ω for a value of $q>k_F$, corresponding to $u_q=0.01$, calculated numerically for $g=1/\ln(100)$. Note the sharp spike just above the bottom of the band which is seen more clearly in the inset.

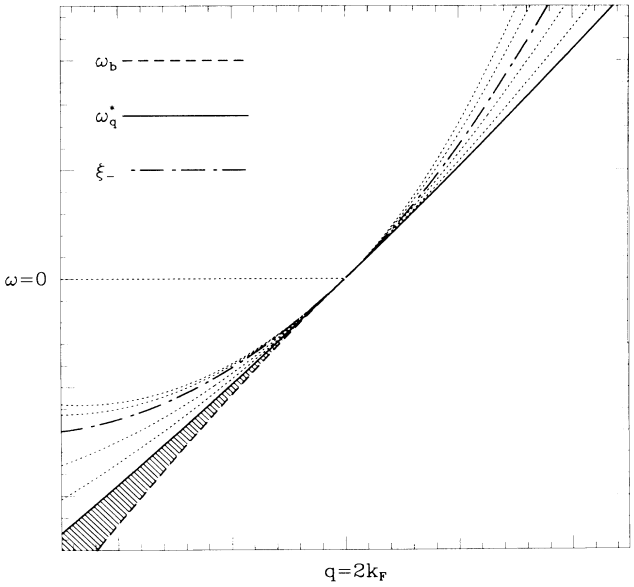

FIG. 9. Schematic contour plot of the phase shift $\delta(q,\omega)$ in the immediate vicinity of $(q=2k_F,\ \omega=0)$, i.e., for q and ω such that $|q-2k_F|\ll 2k_F$ and $|\omega|\ll 2\mu$. The phase shift takes on the value π in the shaded region between the bound-state energy $\omega_b(q)$, denoted by a dashed curve, and the bottom of the two-particle band ω_q^*, denoted by the solid curve. Everywhere else below the bottom of the band, i.e., in the lower right region, $\delta=0$. Within the two-particle band, curves of constant δ are shown by dotted lines, except for the curve $\xi_-(q)$ which is also such a contour but singled out. The phase shift also vanishes along the line $q<2k_F$ and $\omega=0$.

inset. This rather interesting feature appears not to affect the low-energy physics.

We conclude this section with a contour plot of the phase shift in the (q,ω) plane; see Fig. 9. We note that $(2k_F,0)$ is a singular point with the value of δ depending on how that point is approached. From a formal point of view it is most useful to study the vertex part as a function of (complex) ω, for fixed q. From the analogy with potential scattering theory, discussed in the Appendix, one again sees that the bottom of the band is best approached from within the band for fixed q. Thus, for $(2k_F,0)$ we take the limit $\omega\rightarrow 0^+$ for fixed $q=2k_F$. Thus, we conclude that the Fermi-surface $\omega=0$ phase shift vanishes for all q.

V. THERMODYNAMICS

We now consider the thermodynamics of the dilute Fermi gas. Our main aim is to see how the bound states affect quantities like the ground-state energy and the chemical potential, and thus to clarify our interpretation of these states.

Within the ladder approximation, the thermodynamic potential can be expressed in terms of the phase shift through[24]

$$\Omega(\mu)-\Omega_0(\mu)=-\frac{1}{\pi}\sum_{\mathbf{q}}\int_{-\infty}^{+\infty}d\omega\, g(\omega)\delta(\mathbf{q},\omega)\ . \quad (47)$$

Here and below, the subscript 0 denotes the noninteracting system, and the Bose function $g(\omega)=1/[\exp(\beta\omega)-1]$. The chemical potential of the interacting gas is determined by calculating the function $N(\mu)=-\partial\Omega/\partial\mu$ and solving for μ for a given number density of fermions N/L^2.

We note in passing that (47) is the analog of Fumi's theorem for the thermodynamics of a system of noninteracting electrons with impurities. See the Appendix for further discussion of the analogy between the phase shift describing two-body scattering in the dilute Fermi gas, and that of potential scattering theory.

For simplicity, we confine ourselves to $T=0$. The Bose factor $g(\omega)=-1+\Theta(\omega)$, so that the energy integration in (47) runs over $\omega<0$ and the momentum sum over $q\leq 2k_F$. Since the phase shift $\delta(q,\omega)>0$ in this region, as shown in the previous section, we see that $\Omega(\mu)-\Omega_0(\mu)>0$. We now use this fact to prove that the ground-state energy of the system increases due to the interactions.

The change in the ground-state energy, for a fixed density $\bar{N}/L^2$, is

$$E(\bar{N})-E_0(\bar{N})=\Omega(\mu)-\Omega_0(\mu_0)+(\mu-\mu_0)\bar{N}\ , \quad (48)$$

where the chemical potential of the interacting system μ and that of the noninteracting system μ_0 satisfy $\bar{N}=N(\mu)\equiv-(\partial\Omega/\partial\mu)(\mu)$ and $\bar{N}=N_0(\mu_0)\equiv-(\partial\Omega_0/\partial\mu)(\mu_0)$. We substitute $N(\mu)$ for $\bar{N}$ in (48), and then expand the functions $\Omega(\mu)$ and $N(\mu)$ about μ_0. We thus obtain

$$E(\bar{N})-E_0(\bar{N})=\Omega(\mu_0)-\Omega_0(\mu_0)+(\mu-\mu_0)^2\kappa/2+O((\mu-\mu_0)^3)\ , \quad (49)$$

where $\kappa=-\partial^2\Omega/\partial\mu^2|_{\mu_0}=\partial N/\partial\mu|_{\mu_0}>0$ as required by stability. Further, the third-order term is negligible in the dilute limit since the change in the chemical potential due to interactions is controlled by the small parameter g. We thus conclude that the interactions lead to an increase in the ground-state energy. This is important to establish, since it shows that the bound-state poles which appeared below the two-particle band are properly interpreted as excitations and do, in fact, lead to an increase in the ground-state energy.

The contribution of the bound states to (47) comes from ω between the bound-state energy $\omega_b(q)$ and the bottom of the two-particle band ω_q^*; while that from the continuum of scattering states comes from $\omega>\omega_q^*$. This breakup into bound- and scattering state contributions is a bit artificial since we have seen that the existence of the bound state affects the continuum contribution. For instance, the phase shift in the continuum must be π at the bottom of the band in the presence of the bound state. We shall, nevertheless, use the terminology of bound-state and continuum contributions.

At $T=0$, the bound-state contribution is given by

$$\Delta\Omega_b(\mu)=\sum_{q<2k_F}\int_{\omega_b(q)}^{\omega_q^*}d\omega=\frac{4mL^2}{3\pi\hbar^2}\mu^2\exp(-1/g)\ . \quad (50)$$

The resulting change in the density is

$$\Delta N_b(\mu)=-\frac{4mL^2}{\pi\hbar^2}\mu\exp(-1/g)\ , \quad (51)$$

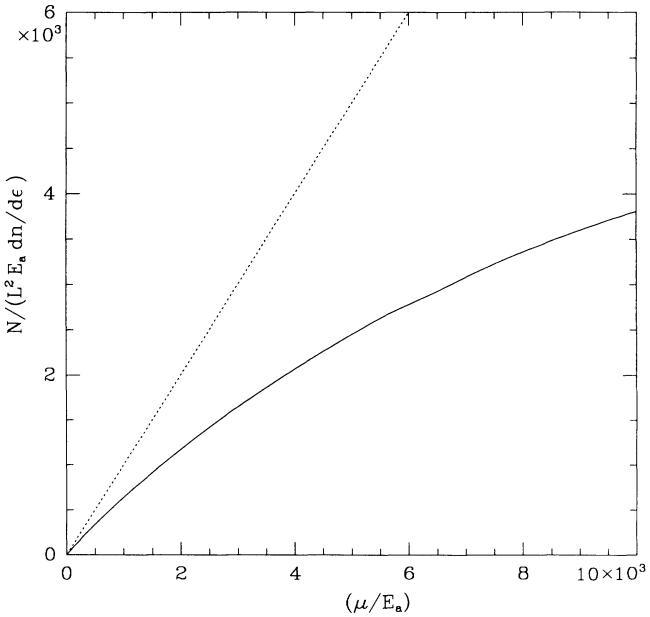

FIG. 10. The number density $N(\mu)$ plotted as a function of the chemical potential μ (where $dn/d\varepsilon=m/\hbar^2$ is the density of states). The noninteracting gas result is the dotted straight line, and the dilute-gas result calculated numerically within our formalism is the solid curve.

where we recall from (15) the μ dependence of g. Since, for a given μ, $\Delta N_b < 0$, for a fixed density of particles the bound states lead to an increase in the chemical potential.

To determine the continuum contribution, the free energy (47) and other thermodynamic quantities requires numerical integration using the phase shifts determined in the previous section. In Fig. 10, we show the results of our numerical calculation of the function $N(\mu)$, which includes both the bound- and continuum state contributions. The solid curve is $N\pi\hbar^2/mL^2$ as a function of μ in units of the energy scale $0.001E_a$, while the dotted line gives the noninteracting solution $N_0\pi\hbar^2/mL^2=\mu$. We see that $N(\mu)<N_0(\mu)$, or equivalently, for fixed N, $\mu>\mu_0$, i.e., repulsive interactions lead to an increase of the chemical potential. We note another feature of the calculation that, for sufficiently large μ/E_a, we find the unphysical result that the compressibility $dN/d\mu<0$. This merely reflects the breakdown of the low-density approximation which, as we have discussed at the end of Sec. II, is only valid for sufficiently large E_a/μ.

VI. SELF ENERGY

We now turn to the question of how the bound states, which are low-lying excitations for q near $2k_F$, affect the single-particle self-energy. In particular, we want to see if the quasiparticles are well defined or not.

The self-energy is obtained from the vertex part $\tilde{\Gamma}$ by joining two of the external legs, as shown in Fig. 11, and is given by

$$\tilde{\Sigma}(\mathbf{p},ip_n)=\sum_{\mathbf{k}}\frac{1}{\beta}\sum_{ik_n}G^0(\mathbf{k},ik_n)\tilde{\Gamma}(\mathbf{p}+\mathbf{k},\,ip_n+ik_n)\ , \tag{52}$$

where the free Green's function $G^0(\mathbf{k},ik_n)=(ik_n-\varepsilon_{\mathbf{k}}+\mu)^{-1}$, and ip_n and ik_n are fermionic Matsubara frequencies. Using the spectral representation

$$\tilde{\Gamma}(\mathbf{q},z)=\int\frac{ds}{\pi}\frac{\Gamma''(\mathbf{q},s)}{s-z}\ , \tag{53}$$

we can evaluate the frequency sum in (52). Analytic continuation in the usual way then leads to the retarded self-energy

$$\Sigma(\mathbf{p},\omega)=-\sum_{\mathbf{q}}\int\frac{ds}{\pi}\frac{[f(\varepsilon_{\mathbf{q}-\mathbf{p}}-\mu)+g(s)]\Gamma''(\mathbf{q},s)}{\omega+\varepsilon_{\mathbf{q}-\mathbf{p}}-\mu-s+i\eta}\ , \tag{54}$$

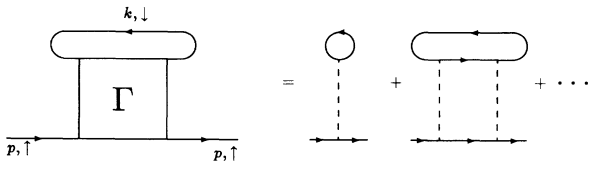

FIG. 11. Self-energy diagrams obtained by closing two of the external lines in Fig. 2 with the same spin and momentum labels.

where f and g are the Fermi and Bose functions, respectively, and we have made the transformation $\mathbf{q}=\mathbf{k}+\mathbf{p}$.

As in the previous section, it is convenient to separate the contributions from the bound state and the continuum of scattering states. This is easy to see in terms of the spectral weight for the vertex part which can be written as

$$\Gamma''(\mathbf{q},\omega)=-\pi R_b(q)\delta[\omega-\omega_b(q)]-\frac{1}{C}\frac{B(\mathbf{q},\omega)}{A^2(\mathbf{q},\omega)+B^2(\mathbf{q},\omega)}\Theta(\omega-\omega_q^*)\ . \tag{55}$$

The δ-function term gives the bound-state pole in Γ with a residue

$$R_b(q)=\frac{-(\omega_q^*)^2}{2C\mu}\exp(-1/g)\ , \tag{56}$$

where $C=mL^2/4\pi\hbar^2$. This follows from expanding (27) about $\omega_b(q)$ to give

$$A(\mathbf{q},\omega)\approx[\omega-\omega_b(q)][-2\mu\exp(1/g)/(\omega_q^*)^2]\ .$$

The second term in (55) comes from the continuum of two-particle states above the bottom of the band ω_q^*.

First we consider the imaginary part of the retarded self-energy $\Sigma''(\omega)$ near the Fermi surface at $T=0$, which is inversely proportional to the quasiparticle lifetime. At the end of this section we discuss the real part and the quasiparticle residue Z.

To second order in g, the continuum contribution, denoted by a subscript c, to the scattering rate at $T=0$ is well known to be

$$\Sigma_c''(k_F,\omega)\sim g^2\mu(\omega/\mu)^2\ln(|\omega|/\mu) \tag{57}$$

as $\omega\to 0$ in two dimensions. The logarithmic correction to the simple ω^2 result arises due to phase-space considerations related to momentum conservation in 2D, as has been pointed out in a golden-rule calculation by Hodges, Smith, and Wilkins.[14] Within a dilute-gas, ladder approximation the above result was obtained by Bloom.[21]

We now wish to see how this result is altered by the bound states. Their contribution to the self-energy, denoted by a subscript b, is obtained by retaining only the δ-function piece of Γ'' in (54). Then, at $T=0$, using $f(x)=\Theta(-x)$ and $g(\omega_b)=-1$, since $\omega_b<0$, we obtain

$$\Sigma_b(\mathbf{p},\omega)=-{\sum_{\mathbf{q}}}'\frac{R_b(q)\Theta(\varepsilon_{\mathbf{q}-\mathbf{p}}-\mu)}{\omega+\varepsilon_{\mathbf{q}-\mathbf{p}}-\mu-\omega_b(q)+i\eta}\ , \tag{58}$$

where the sum is restricted to $q<2k_F$. Its imaginary part is given by

$$\Sigma_b''(\mathbf{p},\omega)=\pi L^2\int\frac{d^2\mathbf{q}}{(2\pi)^2}R_b(q)\Theta(2k_F-q)\Theta[\omega_b(q)-\omega]\times\delta[\omega-\omega_b(q)+\varepsilon_{\mathbf{q}-\mathbf{p}}-\mu]\ . \tag{59}$$

We now have to evaluate this integral for p near k_F and $|\omega|\ll\mu$. The step functions imply that the result is nonzero only for $\omega<\omega_b(q)<0$. Further, only values of q just below $2k_F$ contribute to the integral, so that we may replace $\omega_b(q)$ by ω_q^* to obtain

$$-\frac{\exp(-1/g)}{2\mu}\int_0^{2\mu}d\varepsilon_q\int_0^{2\pi}d\phi(\omega_q^*)^2\Theta(\omega_q^*-\omega)\times\delta(\omega-\omega_q^*+\varepsilon_q+\varepsilon_p-2\sqrt{\varepsilon_q\varepsilon_p}\cos\phi-\mu)\ . \quad (60)$$

We next introduce dimensionless variables $P\ll 1$ and $|\bar{\omega}|\ll 1$ defined by $|\mathbf{p}|=k_F-k_FP$ and $\bar{\omega}=\omega/\mu$. With $x=\omega_q^*/\mu=\varepsilon_q/2\mu-2$, we can rewrite the above result as

$$-\mu\exp(-1/g)\Theta(-\omega)\int_{-|\bar{\omega}|}^{0}dx\int d\phi\, x^2\delta[4+x+\bar{\omega}-2P-4(1+\bar{\omega}/4-P)\cos\phi]\ . \quad (61)$$

The δ function can be further simplified to give

$$\delta[\cos\phi-(1+\bar{\omega}/4+P/2)]/4=\sum_i\delta(\phi-\phi_i)/|4\sin\phi|\ ,$$

where ϕ_i are the two solutions to $\cos\phi=1+\bar{\omega}/4+P/2$. These solutions exist only when $|\bar{\omega}|>2P$ and are given by $\sin\phi_\pm=\pm\sqrt{|\bar{\omega}|/2-P}$. The integrals can now be easily done.

Setting $P=0$ on the Fermi surface, we obtain the bound-state contribution to the self-energy

$$\Sigma_b''(k_F,\omega)=-\frac{\sqrt{2}}{3}\exp(-1/g)\mu|\omega/\mu|^{5/2}\Theta(-\omega)\ , \quad (62)$$

for small ω. Since the bound state consists of two holes, it affects Σ'' only for $\omega<0$, i.e., external hole propagation. The essential singularity in g is characteristic of the bound-state contribution. The singular energy dependence arises from a combination of the limited phase space available for scattering into these states, and of the small spectral weight in the bound pole at low energies.

We see right away that the bound-state contribution is subdominant to the continuum contribution (57) as $\omega\to 0$. Thus, the quasiparticle lifetimes are sufficiently long as one approaches the Fermi surface and these are well-defined excitations of the system.

We conclude this section with a brief discussion of the quasiparticle residue Z which is given by $(1-\partial\Sigma'/\partial\omega)^{-1}$ evaluated at $p=k_F$, $\omega=0$. To compute this quantity for the dilute gas, one can begin with the real part of the self-energy (54) which involves rather more complicated integrals than the analysis of the imaginary part. Since we are only interested in whether Z is nonzero or not, we confine ourselves to some qualitative remarks.

It is clear from (54) that the retarded self-energy has no singularities in the upper half of the ω plane, and thus its real and imaginary parts are related via the Kramers-Kronig relations. It is then easy to see[3] that, for $\Sigma''\sim\omega^2\ln\omega$, Z is nonvanishing.

It may be of some interest to establish the connection[7,8] between Z and the two-body phase shift $\delta(q,\omega)$. Using $\delta=-\tan^{-1}(B/A)$ and $\partial A/\partial(g^{-1})=1$, we find the identity $B/(A^2+B^2)=\partial\delta/\partial(g^{-1})$. Using (55), this allows us to relate the phase shift to the spectral weight in (54).

We note that this relationship between Z and the two-body phase shift in the dilute Fermi gas is not analogous to what is found in the x-ray edge problem.[25] In the latter, the overlap matrix element between the ground states of the noninteracting system in the presence and absence of the impurity potential is proportional to $\exp\{-[\delta(\varepsilon_F)/\pi]^2\ln N\}$. Thus, a nonzero Fermi-surface phase shift (for impurity scattering) leads to a vanishing overlap in the thermodynamic limit. While there are some analogous features to the impurity phase shift and the two-particle shift, which we have discussed in the previous section and in the Appendix, this analogy cannot be apparently carried over to Z.

VII. COMMENTS AND IMPLICATIONS

As explained in the Introduction, the motivation for undertaking this detailed analysis was the possibility of the breakdown in Fermi-liquid theory in two dimensions in view of the anomalous normal-state properties of the high-temperature superconductors. In a regime of low densities where a controlled calculation could be done, we found a negative answer, i.e., that Fermi-liquid theory is resilient.

In this section we comment on the implications of our results and its connections with related work. We first contrast our results with the 1D case, where the breakdown of Fermi-liquid theory is well known. We then turn to a discussion of the normal state of 2D Fermi systems with attractive interactions, where bound states were argued to lead to deviations in Fermi-liquid behavior.

A. One dimension

It is well known[5] that the 1D case is special in that any interaction leads to a state which is qualitatively different from a Fermi liquid. It has been suggested[7,8] that the same may be true of 2D.

Our conclusion is that *if* there is a violation of Fermi-liquid theory in 2D, it is much more subtle than the 1D case; dimensionality alone does not lead to a breakdown of Fermi-liquid behavior in 2D, as it does in 1D.

While a variety of powerful tools have been brought to bear upon the 1D Fermi gas, the only point we wish to discuss here is how the breakdown of Fermi-liquid theory manifests itself in a simple perturbative calculation of the sort presented in this paper.

Consider a second-order perturbation theory calculation of the scattering rate; in terms of self-energy diagrams this corresponds to single particle-hole bubble dressing the propagator, or equivalently the second-order term of Fig. 11. It is easy to show that, in 1D, $\Sigma''(k_F,\omega)\sim\omega$. Phase-space restrictions are responsible for this rather different result from the ones obtained in higher dimensions (ω^2 in 3D and $\omega^2\ln\omega$ in 2D). We should emphasize that this answer is *wrong*.[26] In 1D, both the particle-particle (p-p) and the particle-hole (p-h) channels have logarithms, and a consistent perturbative

calculation requires summing the parquet diagrams. However, even though second-order perturbation theory gives the wrong answer in 1D, it does point to its own inadequacy by showing that the quasiparticles are not well defined.

In contrast, in 2D going to all orders in the p-p channel does not lead to a breakdown of the quasiparticle concept. (The p-h channel does not have a logarithm in the absence of nesting; this allowed us to focus on the p-p channel alone and formulate a consistent low-density expansion.)

B. Attractive Fermi systems

We next turn to a completely different problem: a 2D Fermi system with manifestly *attractive* interactions. Randeria, Duan, and Shieh (RDS) showed that the existence of a bound state in the two-body problem is a necessary and sufficient condition[18,19] for an s-wave pairing instability in a 2D Fermi gas. Thus, the two-body bound states must persist in the normal state; the key question is whether they lead to deviations from Fermi-liquid behavior.

Schmitt-Rink, Varma, and Ruckenstein (SVR) further analyzed the attractive Fermi gas at finite temperatures and showed[20] that bound resonances occur for all center-of-mass momenta $q > 2k_F$. There is a mathematical similarity between these bound pairs of particles and the bound hole pairs with $q < 2k_F$ discussed in this paper; the change in the sign of the inequality being closely related to the change in the sign of the coupling constant g from attractive to repulsive. It should, however, be pointed out that, for sufficiently large q, the SVR bound states are simply those of the two-body problem, and thus persist as $k_F \to 0$. In contrast, the bound states discussed in this paper are collective in that they require $k_F \neq 0$.

The nature of the normal state of the attractive model at intermediate coupling has not yet been satisfactorily understood in our opinion. In addition to the problem of doing an inherently finite-temperature calculation which appears to require numerics, even the validity of the ladder approximation, for the attractive case, has been questioned.[20,27,28] While the mere existence of bound pairs cannot be used as evidence for the breakdown of Fermi-liquid theory, as the calculations in this paper clearly show, the case of attractive interactions differs in an essential way from the one analyzed here.

As pointed out by RDS in the strong-coupling limit of the problem, which can be addressed within the low-density approximation, the normal state is a Bose liquid. Below T_c short coherence length superconductors with $k_F\xi_0 \sim 1$—a striking characteristic of the high-T_c superconductors—are in an intermediate regime[18,19] between the limit of large, overlapping Cooper pairs and the opposite limit of tightly bound composite bosons. Thus, the normal state of such a short coherence length superconductor must, in some sense, be intermediate between the normal states of the two limits, one of which is a Fermi liquid and the other a Bose liquid. The deviations from Fermi-liquid behavior, presumably coming from the existence of some bound pairs in the normal state, have yet to be quantified.

VIII. SUMMARY AND CONCLUSIONS

In this paper we have studied a low-density expansion for the repulsive Fermi gas in 2D. We found an unusual nonperturbative bound-state pole in the particle-particle channel for each center-of-mass momentum $q < 2k_F$. This bound state is characteristic of 2D with a nonzero density of states at the bottom of the two-particle band (in the relative coordinate). It is collective in nature in the sense that it exists only for $k_F \neq 0$, and not in the two-body problem. We have argued that it can be interpreted as an antibound state, or a bound excitation of two holes.

At first sight one might expect such a state to signal the breakdown of Fermi-liquid theory. However, we find this not to be the case. These bound states do not lead to an instability. Furthermore, by studying the imaginary part of the self-energy and the quasiparticle residue, we conclude that the quasiparticle excitations are well defined even in the presence of these bound states. Elsewhere[17] we show that the scattering amplitudes, or the residual interactions between the quasiparticles, are also nonsingular. A controlled calculation within the dilute approximation thus leads to the conclusion that two-dimensionality alone is not sufficient to lead to a breakdown of Fermi-liquid theory.

The effect of the unusual two-hole bound states found in this paper on finite-temperature thermodynamic and transport properties deserves further investigation. From an experimental point of view the most interesting system in which to study these effects would be films of ^{4}He with a low density of ^{3}He atoms.

ACKNOWLEDGMENTS

We would like to thank D. Frenkel, A. J. Leggett, D Loss, T. V. Ramakrishnan, H. T. C. Stoof, S. Trugman, and L. Zhang for useful conversations. We thank P. W. Anderson, E. Abrahams, and A. Ruckenstein for stimulating correspondence and conversations, and H. Fukuyama and D. C. Mattis for sending us results of their work prior to publication. J.R.E. was supported by NSF Grant No. DMR 88-22688. M.R. was supported by the U.S. Department of Energy, Office of Basic Energy Sciences under Contract No. W-31-109-ENG-38.

APPENDIX

In this appendix we discuss some properties of the phase shift $\delta(\mathbf{q},\omega)$, which describes two-particle scattering in the low-density Fermi gas. We emphasize the analogy of this phase shift with its more familiar counterpart in ordinary potential scattering theory. We establish a connection between the phase shift and bound states by proving the analogue of Levinson's theorem (or the Friedel sum rule).

1. Alternative definition of phase shifts

In the text of the paper we have defined the phase shift as the argument of the retarded vertex part:

$$\Gamma(\omega+i\eta)=|\Gamma(\omega)|\exp[i\delta(\omega)] \ . \tag{A1}$$

Here and below we take the center-of-mass momentum $\mathbf{q}$ to have some fixed value and omit it below wherever it is not essential, to simplify the notation.

In analogy with potential scattering theory,[29] we can write down an alternative definition of the phase shift in terms of the two-particle excitation spectrum in a finite box where all states are discrete. We thus define the "scattering phase shift" by

$$\delta_{sc}(\omega_i)=-\pi\frac{(\omega_i-\omega_i^{(0)})}{(\omega_{i+1}^{(0)}-\omega_i^{(0)})} \ , \tag{A2}$$

where the $\omega_i^{(0)}$'s are the two-particle excitation energies of the noninteracting system, and ω_i's those of the interacting system within the ladder approximation. The minus sign ensures that the phase shift is negative for repulsive interactions.

To establish the equivalence of these two definitions, consider the vertex part in the particle-particle channel which is of the form

$$\Gamma(z)=\frac{1}{1/g-\chi(z)} \ . \tag{A3}$$

We study the analytic structure of $\Gamma(z)$ in the complex z plane for a system enclosed in a finite box.

$\Gamma(z)$ has a series of discrete poles on the real z axis whose locations ω_i are given by solutions of

$$\chi(\omega_i)=1/g \ . \tag{A4}$$

Thus, ω_i's are the two-particle excitation energies of the interacting system within a ladder approximation. In addition, $\Gamma(z)$ has a series of zeros on the real axis whose locations $\omega_i^{(0)}$ are given by poles of χ, namely,

$$\frac{1}{\chi(\omega_i^{(0)})}=0 \ . \tag{A5}$$

The $\omega_i^{(0)}$'s are clearly the two-particle excitation energies of the noninteracting system. It is easy to see that the poles and zeros of Γ form an alternating chain along the real axis (see Fig. 2), which, in the infinite volume limit, becomes a branch cut representing the continuum of scattering states.

We can then write the vertex part (still working in a finite box) as

$$\Gamma(z)=W\prod_i\left[\frac{z-\omega_i^{(0)}}{z-\omega_i}\right] , \tag{A6}$$

where W is a real constant. This form will now allow us to use the standard tricks of the Fredholm theory of scattering.[29]

Using the scattering phase shift (A2), one can rewrite (A6) as

$$\Gamma(z)=W\exp\sum_i \ln\left[1-\frac{\delta_{sc}(\omega_i)}{\pi}\frac{(\omega_{i+1}^{(0)}-\omega_i^{(0)})}{(z-\omega_i)}\right] . \tag{A7}$$

Taking the thermodynamic limit, one obtains a branch cut from the bottom of the two-particle band ω_q^* to ∞ along the real axis. For z away from the branch cut, the logarithm in (A7) can be expanded to find

$$\Gamma(z)=W\exp\left[-\int_{\omega_q^*}^{\infty}\frac{d\omega'}{\pi}\frac{\delta_{sc}(\omega')}{z-\omega'}\right] . \tag{A8}$$

Finally, we compute the retarded vertex part with the usual analytic continuation $z\to\omega+i\eta$. We thus obtain

$$\Gamma(\omega+i\eta)$$
$$=W\exp\left[-\mathcal{P}\int_{\omega_q^*}^{\infty}\frac{d\omega'}{\pi}\frac{\delta_{sc}(\omega')}{\omega-\omega'}\right]\exp[i\delta_{sc}(\omega)] , \tag{A9}$$

where $\mathcal{P}$ denotes the principal part. Comparing (A9) and (A1), we immediately obtain the equivalence of the scattering phase shift (A2) and the argument of the vertex part (A1).

2. Levinson's theorem

The analogy with potential scattering theory suggests that there must be a connection between the phase shift at the bottom of the two-particle band (at ω_q^*, corresponding to zero relative momentum for a given q), and the number of bound states n_q peeled off the continuum. We prove that

$$\delta(q,\omega_q^*)=n_q\pi, \quad n_q=0,1,2,\ldots \ . \tag{A10}$$

To prove this result, consider the integral

$$\mathcal{I}=\frac{1}{2\pi i}\int_{\mathcal{C}}dz\frac{d}{dz}\ln\Gamma(q,z) \ . \tag{A11}$$

The contour $\mathcal{C}$ is a circle of infinite radius in the complex z plane which has been deformed to circumvent the branch cut on the real axis from ω_q^* to infinity (see Fig. 12). The contribution from the circle at infinity vanishes and we obtain

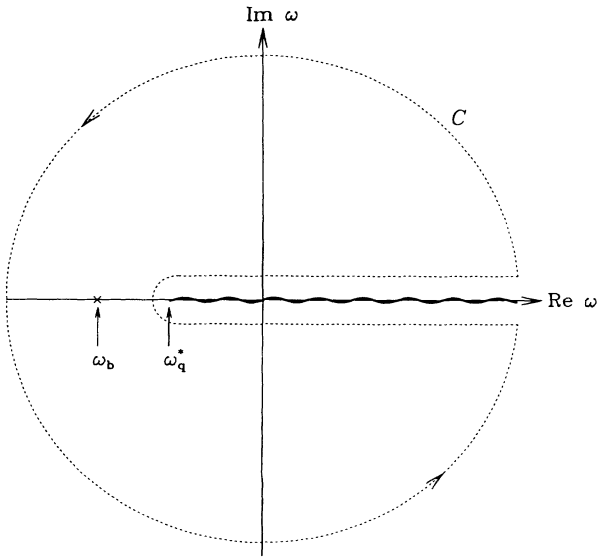

FIG. 12. The contour $\mathcal{C}$ used in the proof of Levinson's theorem. In the complex ω plane, the vertex part Γ has a branch cut along the real axis starting at ω_q^*, for each $\mathbf{q}$, and also an isolated pole at $\omega_b(q)$ for $q<2k_F$.

$$\mathcal{I}=\frac{1}{2\pi i}\int_{\omega_q^*}^{\infty}d\omega\frac{d}{d\omega}[\ln\Gamma(q,\omega+i\eta)-\ln\Gamma(q,\omega-i\eta)]\ . \tag{A12}$$

Since $\Gamma(q,\omega\pm i\eta)=|\Gamma|\exp(\pm i\delta)$ above and below the branch cut, we obtain

$$\mathcal{I}=-\delta(q,\omega_q^*)/\pi\ , \tag{A13}$$

where we have used $\delta(q,\omega)=0$ as $\omega\to\infty$.

By deforming the contour in (A11) it is easy to see that $\mathcal{I}$ counts the number of zeros (located at two-particle excitation energies in the noninteracting system) minus the number of poles (located at two-particle excitation energies in the interacting system) of $\Gamma(q,z)$ enclosed within $\mathcal{C}$. The only two-particle states outside the continuum are bound states below the band, if they exist. (We are assuming here that there is no instability which would give rise to poles off the real axis.) The contribution of these isolated poles gives $\mathcal{I}=-n_q$, which together with (A13) leads to the result (A10).

[1]J. Bednorz and K. A. Müller, Z. Phys. B **64**, 189 (1986); M. K. Wu *et al.*, Phys. Rev. Lett. **58**, 908 (1987).

[2]P. W. Anderson, Science **235**, 1196 (1987); in *Frontiers and Borderlines in Many Particle Physics,* Proceedings of the International School of Physics "Enrico Fermi," Course CIV, edited by R. A. Broglia and J. R. Schrieffer (North-Holland, Amsterdam, 1988).

[3]C. M. Varma, P. Littlewood, S. Schmitt-Rink, E. Abrahams, and A. Ruckenstein, Phys. Rev. Lett. **63**, 1996 (1989).

[4]See, *High Temperature Superconductivity,* Proceedings of the Los Alamos Conference, edited by K. Bedell *et al.* (Addison-Wesley, Reading, MA, 1990).

[5]V. J. Emery, in *Highly Conducting One-Dimensional Solids,* edited by J. T. Devreese *et al.* (Plenum, New York, 1979); J. Solyom, Adv. Phys. **28**, 201 (1979).

[6]F. D. M. Haldane, J. Phys. C **14**, 2585 (1981).

[7]P. W. Anderson, Phys. Rev. Lett. **64**, 1839 (1990); P. W. Anderson and Y. Ren, in *High Temperature Superconductivity* (Ref. 4).

[8]P. W. Anderson, Phys. Rev. Lett. **65**, 2306 (1990).

[9]J. R. Engelbrecht and M. Randeria, Phys. Rev. Lett. **65**, 1032 (1990).

[10]J. R. Engelbrecht and M. Randeria, Phys. Rev. Lett. **66**, 3325 (1991).

[11]V. M. Galitskii, Zh. Eksp. Teor. Fiz. **34**, 151 (1958) [Sov. Phys. JETP **7**, 104 (1958)]. For a pedagogical treatment see, A. Fetter and J. Walecka, *Quantum Theory of Many Particle Systems* (McGraw-Hill, New York, 1971), Sec. 11.

[12]K. Huang and C. N. Yang, Phys. Rev. **105**, 767 (1957); T. D. Lee and C. N. Yang, *ibid.* **105**, 1119 (1957).

[13]A. A. Abrikosov and I. M. Khalatnikov, Prog. Rep. Phys. **22**, 329 (1959), Appendix A1 and references therein.

[14]C. Hodges, H. Smith, and J. W. Wilkins, Phys. Rev. B **4**, 302 (1971).

[15]H. Fukuyama, O. Narikiyo, and Y. Hasegawa, J. Phys. Soc. Jpn. **60**, 372 (1991); **60**, 2013 (1991).

[16]D. C. Mattis and H. Chen (unpublished).

[17]J. R. Engelbrecht, M. Randeria, and L. Zhang, Phys. Rev. B. **45**, 10 135 (1992).

[18]M. Randeria, J. Duan, and L. Shieh, Phys. Rev. Lett. **62**, 981 (1989).

[19]M. Randeria, J. Duan, and L. Shieh, Phys. Rev. B **41**, 327 (1990).

[20]S. Schmitt-Rink, C. M. Varma, and A. Ruckenstein, Phys. Rev. Lett. **63**, 445 (1989).

[21]P. Bloom, Phys. Rev. B **12**, 125 (1975).

[22]The equations of this subsection are valid for *all* q and generalize those given earlier in Ref. 9, which were applicable only for the range $q\leq 2k_F$ of interest in that paper.

[23]This is an example of the result obtained in Sec. 20 of A. A. Abrikosov, L. P. Gorkov, and I. E. Dzyaloshinski, *Methods of Quantum Field Theory in Statistical Mechanics* (Dover, New York, 1975). This logarithmic singularity at the Fermi surface leads to superconductivity for attractive interactions.

[24]P. Nozières and S. Schmitt-Rink, J. Low Temp. Phys. **59**, 195 (1985).

[25]P. W. Anderson, Phys. Rev. Lett. **18**, 1049 (1967).

[26]The Kramers-Kronig transform of $\Sigma''(\omega)\sim\omega$ gives a real part which would lead to Z vanishing logarithmically, whereas the correct 1D result for Z has a power-law singularity at the Fermi surface.

[27]J. Serene, Phys. Rev. B **40**, 10 873 (1989).

[28]A. Tokumitu, K. Miyake, and K. Tamada, J. Phys. Soc. Jpn. **60**, 380 (1991).

[29]K. Gottfried, *Quantum Mechanics* (Benjamin, New York, 1966), Vol. I, Sec. 49.